Key Engineering Materials Vol. 443 (2010) pp 433-438
Online available since 2010/Jun/02 at www.scientific.net
© (2010) Trans Tech Publications, Switzerland
doi:10.4028/www.scientific.net/KEM.443.433

Chipping Brittle Materials: A Finite Element Analysis

Seyed Saleh Mostafavi[1,a], L.C. Zhang[1,b] and Jason Lunn[2,c]

[1]School of Mechanical and Manufacturing Engineering,
The University of New South Wales, NSW 2052, Australia

[2]Bradken, 2 Maud Street, Mayfield West, NSW, 2052, Australia

[a]s.mostafavi@student.unsw.edu.au, [b]Liangchi.Zhang@unsw.edu.au, [c]jlunn@bradken.com.au

Keywords: Edge chipping; Brittle material; Damage modeling

Abstract. Edge chipping by an indenter has been used to investigate the fragmentation of brittle materials. This paper proposed a constitutive model for studying both the initiation and propagation of cracks during the chipping of concrete. The analysis was carried out by the finite element method using a commercially available code, LS-DYNA. The results showed that a zone with very high compressive stresses appears beneath the indenter and causes the material to break or crush. Most of the external work, about 78%, was dissipated in the crushing zone while only a small percentage (less than 17%) contributed to form chips/fragments. As the indentation proceeded, radian-median cracks initiated and propagated downward and parallel to the front surface of the material to form a half penny crack. The crack tips from both sides of the indenter on the surface would then deviate toward the free edge, leading to a chipping scallop at a critical load.

Introduction

In edge chipping, a concentrated load is applied near the edge of a brittle material, as shown in Fig. 1, which may lead to premature chipping [1]. Such an edge chipping test has been investigated by a number of researchers because the cutting of brittle materials, e.g., in coal mining using a long wall shearer, can be roughly regarded as a series cycles of edge chipping, of which each consists of a crushing and chipping phase. An edge chipping process can also be used to understand the properties of brittle materials (e.g., toughness) [1] and provide insight for machining technique development [2] and device design [3]. Figure 1 shows a chip formed in an edge chipping experiment where d_c is the depth of cut which is the distance from indenter tip to the edge of the specimen, H is the chip height, and L is its length.

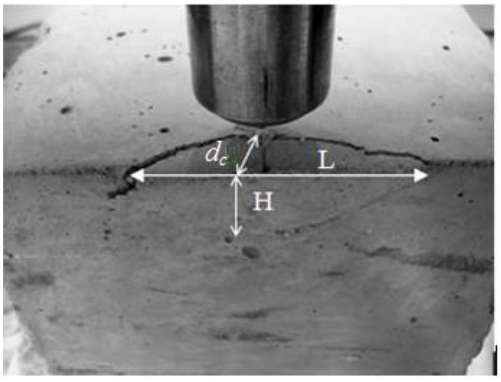

Fig. 1 A chipping test and the geometry of a chip.

Several attempts have been made to understand the relationship of critical chipping load P_F, chip dimensions (d_c, H and L) and material properties. However, to carry out a numerical analysis of the chipping process, it is essential to have a constitutive model to describe the material behavior under severe hydrostatic stresses followed by crack initiation and propagation [4, 5]. This paper will

All rights reserved. No part of contents of this paper may be reproduced or transmitted in any form or by any means without the written permission of TTP, www.ttp.net. (ID: 129.94.206.63-02/08/12,02:46:12)

propose a constitutive model that can integrate with damage development to investigate the edge chipping.

Theory of the Constitutive Model

The continuous surface cap model (CSCM) in the materials library of LS-DYNA is appropriate for brittle materials like rocks or concrete. It can be used to integrate with damage development to describe deformation and fragmentation in a brittle material.

The strength surface in CSCM is formulated in terms of three stress invariants, J_1, J_2' and J_3', which are defined, in terms of the deviatoric stress tensor S_{ij} and pressure P, as

$$J_1 = 3P\ ,\ J_2' = \frac{1}{2}S_{ij}S_{ij}\ ,\ J_3' = \frac{1}{3}S_{ij}S_{jk}S_{ki}\ . \tag{1}$$

The plasticity surface in CSCM blends the shear surface and cap hardening surface to form a smooth intersection. The equation of the plasticity surface is based on the three invariants and the cap hardening parameter, k, i.e.,

$$f(J_1, J_2', J_3', k) = J_2' - \Re^2 F_f^2 F_c \tag{2}$$

where F_f is the equation of the shear failure surface, F_c is the equation of hardening cap, and $\Re$ is the Rubin three-invariant reduction function determining the strength for any state of stress relative to the strength in a triaxial compression test [6].

Within the failure surface, a material is assumed to be isotropic and elastic, govern by the following equation [6]:

$$\Delta\sigma_{ij}^{\ e} = (k - 2/3G)\Delta\varepsilon_{kk}^{\ e}.\delta_{ij} + 2G\Delta\varepsilon \tag{3}$$

The trial stresses and invariants are computed from Eq. (3) to form $f(J_1, J_2', J_3', k)$. If $f(J_1, J_2', J_3', k) \le 0$, then the trial stresses are final; otherwise if $f(J_1, J_2', J_3', k) > 0$, the plastic consistency and flow rule are invoked and the plastic strains and stresses must be re-calculated based on the plastic flow rule. This iteration continues until $f(J_1, J_2', J_3', k) \le 0$ is satisfied.

Damage Model

Two types of damages will be integrated with the CSCM: (a) the ductile damage which accumulates when the mean stress is compressive and the strain energy exceeds the damage threshold τ_{0c}, and (b) the brittle damage which accumulates when the mean stress is tensile and the strain energy exceeds the damage threshold τ_{0t}, where the strain energies of the ductile and brittle damages are defined below:

$$\tau_c = \sqrt{\frac{1}{2}\sigma_{ij}\varepsilon_{ij}} \tag{4}$$

$$\tau_t = \sqrt{K\varepsilon_v^2} \tag{5}$$

The initial damage threshold is coincident with the shear failure surface F_f defined in Eq. (2). The stresses are first obtained without considering the damage. They will then be degraded based on a scalar damage parameter, d, by

$$\bar{\sigma}_{ij} = (1-d)\sigma_{ij} \tag{6}$$

Where $\bar{\sigma}_{ij}$ is the damaged stress and d is the maximum of the ductile and brittle damage defined by Ref. [6]

$$d(\tau_c) = \frac{0.999}{B}\left[\frac{1+B}{1+B\exp(-A(\tau_c - \tau_{0c}))} - 1\right] \tag{7}$$

$$d(\tau_t) = \frac{0.999}{D}\left[\frac{1+D}{1+D\exp(-C(\tau_t - \tau_{0t}))} - 1\right] \tag{8}$$

In Eq. (6), $d = 0$ corresponds to the undamaged or uncracked state and $d = 1$ defines the complete failure. Using LS-DYNA, either brittle or ductile damage contours can be obtained to show the distribution and shape of a damaged zone. Alternatively, an erosion algorithm can be used to delete elements with damage value more than a critical value (defined by the user) to show separation/fracture. In Eqs. (7) and (8), A, B, C and D, determined by experiment, define the shape of softening in stress-displacement or stress-strain curves.

There are two methods for setting up the CSCM input parameters. The traditional method is to supply all material parameters, such as moduli, strengths, hardening, softening, and rate effects parameters. The other, which is more convenient, is to use the default parameters for concrete based on three input specifications: the unconfined compression strength, the aggregate size, and the units. To calibrate the damage model, experimental data from an unconfined compression test are required, of which the details can be found in [7]. Table 1 lists the properties of concrete used in the present study.

Table 1 Some mechanical properties of the concrete specimen.

Density [g/cm^3]	Elastic Modulus [GPa]	Shear Modulus [GPa]	Bulk Modulus [GPa]	Poison's Ratio	Uniaxial Compressive Strength [MPa]	Uniaxial Tensile Strength [MPa]
2.3	34	15.52	13.89	0.2	48	5

Experiment Setup

The specimen used in experiment was a block of concrete of dimensions 150×150×150 mm. The mechanical properties of the material are listed in Table 1. The edge chipping tests were carried out on an INSTRON 5567 machine at the loading speed of 1mm/min using a pyramid indenter of tungsten carbide shown in Fig. 2. The depth of cut d_c was 5mm as shown in Fig. 1.

Fig. 2 The pyramidal indenter used in experiment.

Boundary Condition and the FE Model

The control volume of the FE model was 35×50×35 mm, consisting of 260,615 constant stress solid elements. To characterize the damage deformation, no symmetric conditions can be used for both the specimen and indenter. In order to prevent zero deformation modes (Hourglassing) in the elements, the Hourglass control card of Type 1 with coefficient of 0.05 was applied. The lower surface of the control volume was constrained in all degrees of freedom but the rest of the surfaces were free. The indenter was moved down vertically at a speed of 1.5mm/sec. The contact between the indenter and the specimen was modeled by the automatic surface-to-surface contact in LS-DYNA. To avoid any artificial material interpenetration, the contact formulation of Type = Soft 1 and contact thickness of 0.1mm was used. The coefficient of friction was taken as 0.6.

Results and Discussion

The FEA results show that a zone with very high compressive stresses appears beneath the indenter (Fig. 3). It is therefore expected that the material in this zone will be broken or crushed.

As the indentation proceeds, the crushed zone expands to the surrounding region until the maximum tensile stress in the outer region is high enough to initiate cracking. In the literature, there are some different explanations about the mechanisms of chipping. Some authors proposed that chipping crack is a tensile crack and some others argued that it is a shear or mixed mode crack [8]. The mechanism can now be clarified by our numerical simulations to be described below. Figures 4 and 5 represent the development of the damages at different stages of the indenter penetration during edge chipping.

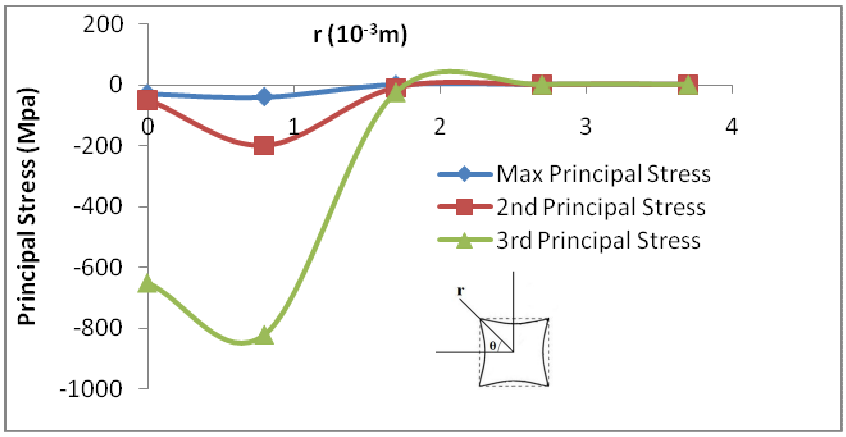

Fig. 3 Principal stresses in the specimen material surface in contact with the indenter at the indentation depth of δ = 0.75 mm at which the radius of contact at θ = 45° is a = 1.49 mm.

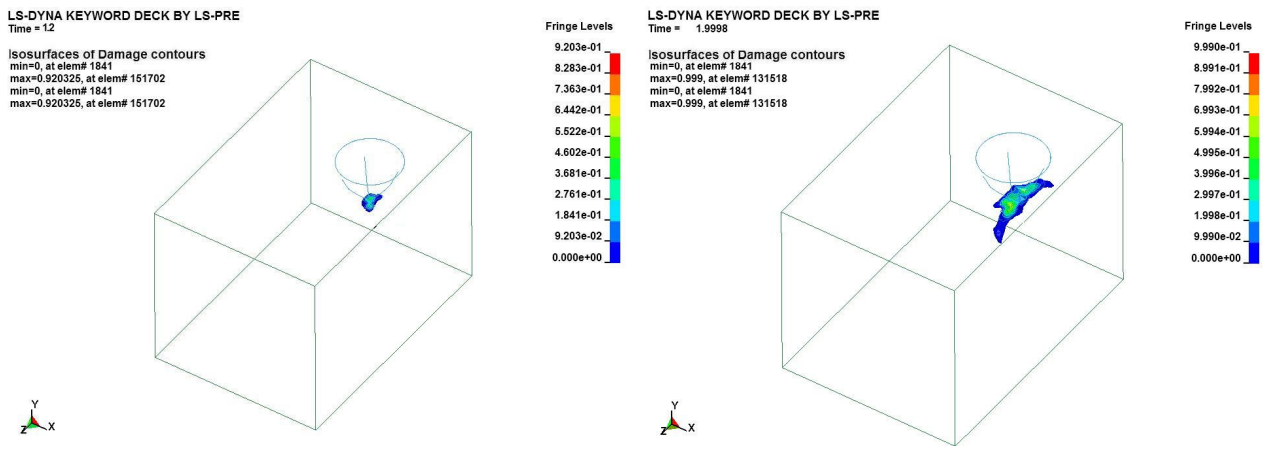

Fig. 4 Isosurfaces of the damage contours, initiation of damage zone in the early stage of the indentation at time t = 1.2s (left), and propagation of cracks parallel to free surface at t = 2s (right).

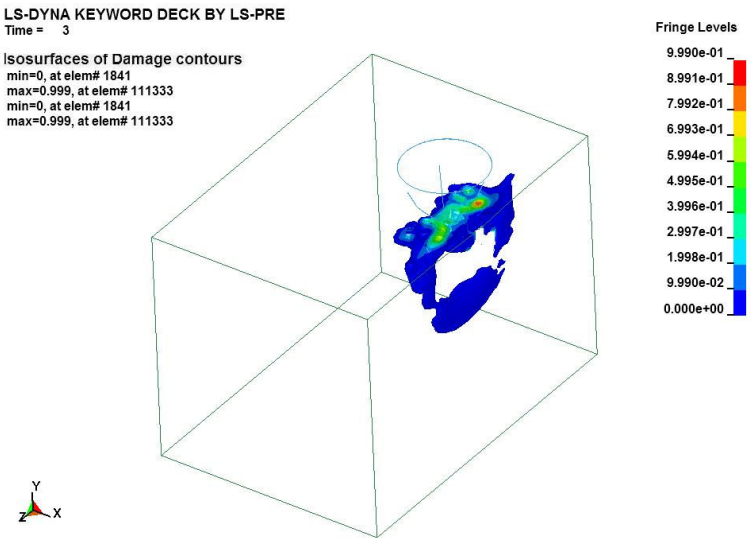

Fig. 5 Evolution of a penny-shape crack and its propagation towards the free edge (t = 3 s).

When the indenter penetrates further, the radian-median cracks propagate, form a half penny crack, and finally intersect to lead to the chipping of the material. Figure 6 compares an FEA prediction with an experimental observation. They are in very good agreement.

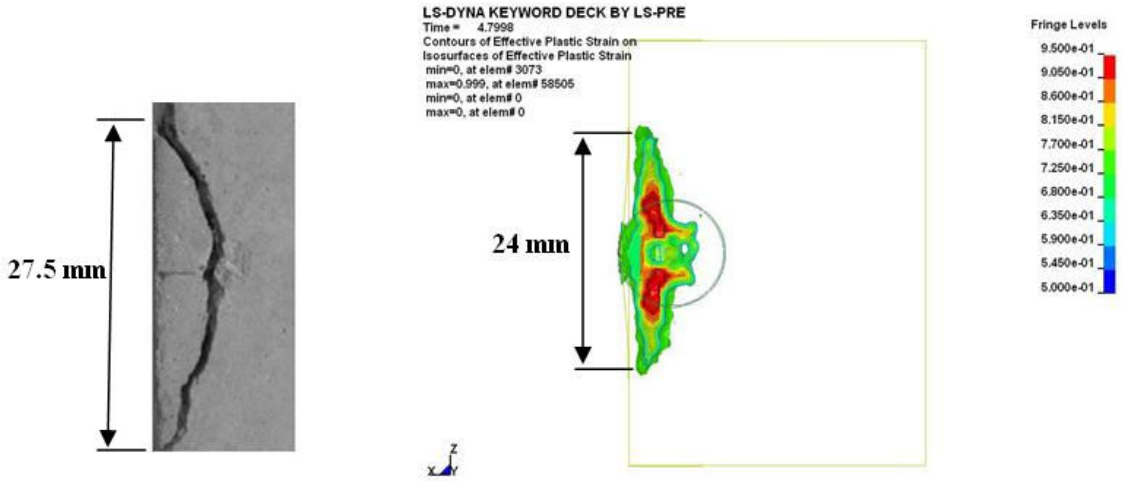

Fig. 6 Top view of the crack and the chip formation in edge chipping experiment (left) and the damaged zone in modelling (right).

The fraction of the energy consumed by crushing deformation is a good indication to assess the efficiency of a chipping process. In coal mining, for instance, if most of the external work done by the indenter is dissipated in forming the crushed zone, the cutting would be considered inefficient because it produces more small particles which contribute to dust generation. To measure the fraction of the energy consumed in the crushed zone, we can analyze a loading-unloading up to the critical indentation depth of $\delta = 0.825$ mm beyond which chipping occurs. As shown in Fig. 7, the energy consumed by crushing is the area within the loading-unloading curve, i.e., area *OAB*. The elastic energy that will release after unloading is represented by area *ABC*.

It was found that the amount of energy which goes to crushing is about 0.5J but that of elastic strain energy is about 0.032J. When the indenter keeps loading further to point *F*, edge chipping occurs. Up to this stage, the total work done was found to be 0.64J. Hence, more than 78% of the external work dissipates in crushing, less than 17% of the total energy contributes to create major cracks to bring about the chipping, and about 5% is the released elastic energy.

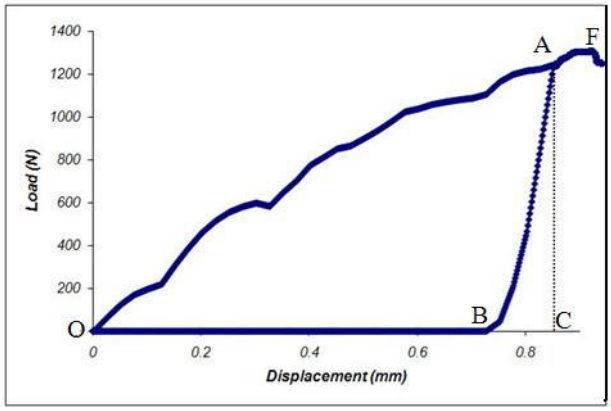

Fig. 7 The force-Displacement curve in an indentation cycle just before chipping.

Conclusions

This paper proposed a constitutive model that integrates the continuous surface cap model with damage generation to study the initiation and propagation of cracks during the chipping of concrete. The major findings are as follows:

(a) Most of the external work, about 78%, was dissipated in the crushing zone, which is not favourable in many applications such as coal mining, because this large portion of the energy was consumed in the production of small particles, a main source of dust generation in coal mining.

(b) The finite element simulation provides a clear figure of the chipping process. As the indentation proceeds, radian-median cracks initiate and propagate downward and parallel to the front surface to form half penny cracks. The crack tips from both sides of the indenter on the surface will then extend toward the free edge, leading to a chipping scallop.

Acknowledgement

The work has been supported by the Australian Research Council and BRADKEN®.

References

[1] H. Chai and B.Lawn: Acta Material 55 (2007), p.2555

[2] Quinn J, Su L, Flanders L and Lloyd: Machining science and technology 4(2) (2000), p.291

[3] R. Danzer, M. Hangl, and R.Paar: Ceramic Trans., Vol. 122 (2001), p.43

[4] Y. Tang, A. Yonezu, N. Ogasawara, N. Chiba and X. Chen: Proc. R. Soc. A 464 (2008), p.2967

[5] J. Yan, A.M. Karlsson and X. Chen: Engineering fracture mechanics 74 (2007), p.2535

[6] LS-Dyna Keyword Manual, Version 971, LSTC, CA (May 2007)

[7] Len Schwer: Demonstration Continuous surface Cap Model with Damage Calibration, SE&CS (2003)

[8] H. W.G.M. Van Kersteren, in: *Proceeding of fracture of brittle, disordered materials*, edited by G.Baker, B.L. Karihalloo (Sep 1993)

Advances in Materials Processing IX
10.4028/www.scientific.net/KEM.443

Chipping Brittle Materials: A Finite Element Analysis
10.4028/www.scientific.net/KEM.443.433

DOI References
[1] H. Chai and B.Lawn: Acta Material 55 (2007), p.2555
doi:10.1016/j.actamat.2006.10.061

[2] Quinn J, Su L, Flanders L and Lloyd: Machining science and technology 4(2) (2000), p.291
doi:10.1080/10940340008945711

[4] Y. Tang, A. Yonezu, N. Ogasawara, N. Chiba and X. Chen: Proc. R. Soc. A 464 (2008), p.2967
doi:10.1098/rspa.2008.0077

[5] J. Yan, A.M. Karlsson and X. Chen: Engineering fracture mechanics 74 (2007), p.2535
doi:10.1016/j.engfracmech.2006.12.005